



Fabrication and characterization of Sb-doped MXene prepared by hydrothermal method for use as a sensing electrode for heavy metal detection

Siranaree PHOOHADSUAN¹, Thitima Maturros DANIELS², Mati HORPRATHUM², Nichaphat THONGSAI¹, and Eakkasit PUNRAT^{1,*}

¹ Department of Chemistry, Faculty of Science, Ramkhamhaeng University, Bang Kapi, Bangkok, 10240, Thailand

² Opto-Electrochemical Technology, National Electronics and Computer Technology Center, Pathum Thani, 12120, Thailand

*Corresponding author e-mail: eakkasit.p@ru.ac.th

Received date:
25 March 2024

Revised date
11 April 2024

Accepted date:
17 May 2024

Keywords:

Antimony;
Electrochemical sensor;
Heavy metal detection;
Hydrothermal;
MXene

Abstract

MXene, a two-dimensional material with favorable physicochemical characteristics, has demonstrated outstanding efficiency in a wide range of applications because of their superior properties, such as higher surface area and conductivity, and facile surface modification. In this study, antimony (Sb) doped MXenes were synthesized via a simple hydrothermal method, employing various Sb concentrations ranging from 5%w/w to 25%w/w. The successful preparation of the Sb-doped MXene (Sb@MXene) was confirmed by an X-ray diffraction (XRD) method. Physical morphologies examined through field-emission scanning electron microscopy (FE-SEM) depict the presence of Sb nanoparticles with the size of about 80 nm on the surface and interlayer of MXenes. The Sb@MXene composites demonstrated significant potential as electrochemical sensing materials for heavy metal detection. Both 5%Sb@MXene and 25%Sb@MXene composites were prepared as the screen-printed electrode (SPE) materials via drop-casting method to sense Pb²⁺, Cd²⁺, and Zn²⁺. The 25%Sb@MXene SPE show the highest sensitivity toward Pb²⁺ (3.62 $\mu\text{A}\cdot\text{ppm}^{-1}$), Cd²⁺ (2.53 $\mu\text{A}\cdot\text{ppm}^{-1}$), and Zn²⁺ (0.90 $\mu\text{A}\cdot\text{ppm}^{-1}$) solution, compared with that of 5%Sb@MXene SPE. This work not only demonstrates a simple preparation of Sb@MXene, but also applies the hybrid materials in electrochemical sensing application.

1. Introduction

In recent years, the exploration and development of advanced materials have grown increasingly important to meet the changing demands of diverse technological applications. MXene, a new class of two-dimensional (2D) transition metal carbides, nitrides, and carbonitrides, has gained prominence among these materials due to their remarkable mechanical, electrical, and thermal properties [1]. $\text{M}_{n+1}\text{X}_n\text{T}_x$ is the generic formula for MXene, where M is the early transition metal, for example, titanium (Ti), Molybdenum (Mo), Scandium (Sc), and Vanadium (V). X stands for carbon (C) or nitrogen (N). T_x is the symbol for the functional groups (such as $-\text{OH}$, $-\text{F}$, $=\text{O}$, etc.) that are adhered to the surface of the compound as a result of etching the MAX phase [2]. MXenes are generally prepared via HF etching in which loosely stacked MX layers after removing A-layer atoms (normally group IIIA and IVA elements) from the MAX phases, a class of layered ternary carbides and nitrides with a hexagonal structure [3]. MXenes have attracted significant attention for a variety of applications, including as energy storage, catalysis, sensor, electrical device, and biomedical applications due to their unique combination of high conductivity, high surface area, hydrophilicity, and exceptional chemical stability [4-6].

Superior surface modifications of 2D materials using a special synthesis process provide the benefit of different morphologies,

increased surface area, and surface functions [7]. "Doping," or adding foreign elements is one of the most useful techniques for adjusting the chemical and physical characteristics of the 2D materials. The surface functionalization by doping heteroatoms on the 2D lattice structure is therefore an effective way to develop the performance of MXenes [8]. For instance, Qu *et al.* developed a straightforward phosphorization method to introduce oxygen and phosphorus to Mo_2CT_x MXenes. Compared with the undoped-MXenes, the phosphorus-doped MXenes have noticeably better conductivity and electrocatalytic performance toward the hydrogen evolution reaction [9].

Among the diverse range of dopants investigated, antimony (Sb) doping has garnered significant attention due to its potential to introduce additional functionalities and tune the electronic properties of MXenes. For example, Thirumal *et al.* prepared MXene@Sb nanoneedle nanocomposite using a hydrothermal treatment. The as-prepared nanocomposite demonstrated high photocatalytic activity for methylene blue and rhodamine B degradation [10]. Arnold *et al.* fabricated antimony/MXene hybrid electrodes for sodium-ion batteries [11]. The incorporation of Sb into MXene structures has been shown to impact the material's electronic band structure, thereby improving its conductivity and catalytic activity [10,11]. As reported in previous works, among the most adaptable and efficient post-modification of MXenes is hydrothermal synthesis. The hydrothermal method produces extremely crystalline structures with well-defined reaction

conditions that are highly controlled. Furthermore, this technique provided the advantage of scalability and reproducibility for producing Sb-doped MXenes with unique properties [12,13].

Nowadays, the detection of heavy metal has attracted a lot of interest in sensing applications because it can pollute a range of environmental natural resources. Some extremely poisonous heavy metals including lead (Pb), cadmium (Cd), zinc (Zn), and mercury (Hg), have the potential to seriously harm aquatic life, humans, and ecosystems [14-16]. Because the surface functional groups presented in MXenes allows them to have greater compatibility with other substrates and unique electronic properties, compared with other 2D materials, the MXene would be a promising candidate for electrochemical sensing of heavy metals. In addition, Sb film electrodes prepared by the modification on glassy carbon electrodes have been developed for voltametric sensing of heavy metals due to its weak oxidation signal, which made it possible to detect analytes whose oxidation potentials were near to those of Sb [17,18]. The Sb-doped MXene electrode is therefore promising candidate for detecting heavy metal using simultaneous electrochemical analysis.

Nevertheless, the multilayered structure of MXenes with its narrow interlayer spacing limits the electrode performance as reducing the electroactive sites on the materials. Doping is thus an effective way to increase MXene's layer distance for improving sensing performance [14]. For instance, He *et al.* synthesized and applied bismuth/MXene nanocomposite for glassy carbon electrode (GCE) materials. Due to its high surface area and conductivity, the as-prepared nanocomposite-modified GCE in electrochemical sensing system exhibited high sensitivity toward Pb^{2+} and Cd^{2+} [19].

The purpose of this work is thus to investigate the simple preparation and structural characterization of the Sb-doped MXene composites via the hydrothermal method. The integration of Sb into the MXene structure was confirmed by X-ray diffractometry (XRD), field-emission scanning electron microscopy (FE-SEM), and electron dispersion spectroscopy (EDS). In addition to structural and morphological investigations, for the first time, the Sb-doped MXene composites were utilized as a screen-printed electrode (SPE) materials for electrochemical sensing, especially those involving the detection of heavy metals including Pb^{2+} , Cd^{2+} and Zn^{2+} (Figure 1). These results not only highlight the potential of Sb-doped MXene as an effective electro-

chemical sensing material electrode, but also demonstrate the wider field of material design for further advanced applications.

2. Experimental

2.1 Chemicals and materials

Titanium aluminum carbide powder (Ti_3AlC_2 , MAX phase) with a particle size of 400 mesh and a purity exceeding 99% was supplied from Luoyang Advanced Material Co., Ltd., China. Lithium fluoride (LiF), sodium chloride (NaCl), and antimony (Sb) powder were sourced from Sigma-Aldrich, Denmark. Potassium ferricyanide ($K_3[Fe(CN)_6]$) was obtained from Fluka-Garantie, Germany. Potassium ferrocyanide ($K_4[Fe(CN)_6]$) was purchased from Ajax Chemical, Australia. Lead ($Pb(NO_3)_2$), cadmium nitrate tetrahydrate ($Cd(NO_3)_2$), and zinc chloride ($ZnCl_2$) with a purity exceeding 99% were sourced from Sigma-Aldrich, Denmark. These heavy metals have been studied and utilized in electrochemical detection due to their distinctive electrochemical properties. Deionized (DI) water was used throughout all experiments.

2.2 Preparation of MXenes and Sb@MXene

MXenes were synthesized by selectively removing aluminum from the MAX phase (Ti_3AlC_2) through chemical etching, employing an *in-situ* HF formation facilitated by LiF mixed with HCl. In this process, 1 g of Ti_3AlC_2 powder was gradually added over a 5 min period to a 20 mL etchant solution consisting of 12 M LiF in HCl. The mixed solution was stirred with a Teflon magnetic bar at room temperature ($\sim 23^\circ C$) for 24 h. Subsequently, the solution underwent washing with DI water through centrifugation at 3500 rpm for 5 min. After each centrifuge cycle, Ti_3AlC_2 powder settled at the tube's bottom as sediment, separated from the water-like supernatant. The sedimented Ti_3AlC_2 was redispersed in an additional 150 mL of DI water, followed by another centrifugation cycle. The washing cycles were repeated until the pH of the supernatant reached approximately 6. The Ti_3AlC_2 sediments were then dried in a vacuum oven at $70^\circ C$ for 24 h, and the resulting powder was stored in the refrigerator before further experiments.

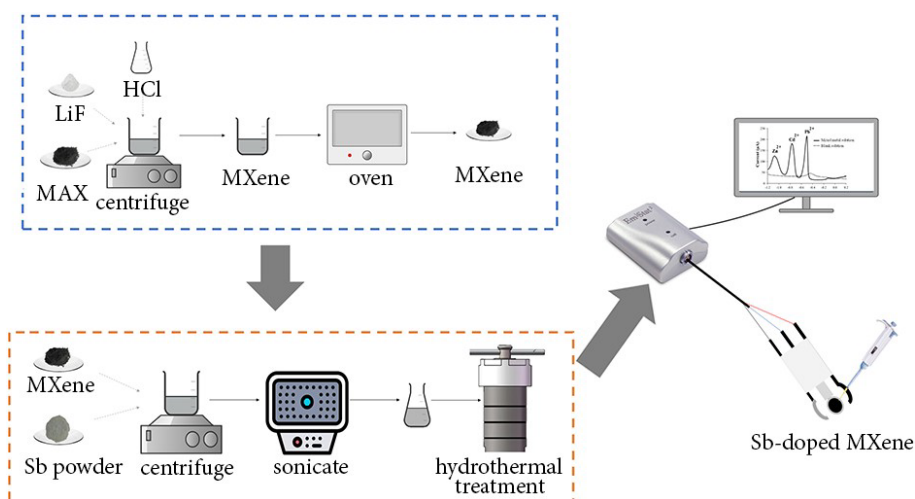


Figure 1. Schematic illustration of Sb@MXene SPE fabrication.

To prepare the Sb-doped MXene (Sb@MXene) composites, the growth of antimony nanoparticles on few-layered MXene hybrid composites was achieved using a single-step hydrothermal method. Initially, 0.5 g of the as-prepared MXenes ($\text{Ti}_3\text{C}_2\text{T}_x$) were suspended in 50 mL of DI water. Subsequently, 0.25 g and 0.125 g (5 wt% and 25 wt%) of Sb powder was slowly added with constant stirring and ultrasonic treatment for 1 h. The Sb@MXene composite was then produced using the hydrothermal treatment in an autoclave at 150°C for 12 h. Finally, the resulting sponge-like black powder was filtered using a Whatman filter paper (0.2 μm pore size).

2.3 Structural and morphology characterization

The morphologies of both pristine MXenes and Sb-doped MXenes were observed using a field-emission scanning electron microscope (FE-SEM: Hitachi, SU8030), operating at an accelerating voltage of 10 kV and a working distance of 8.0 mm. An X-ray diffractometer (XRD: PANalytical) was employed to study the crystalline structure of the materials. The data were recorded using a $\text{Cu K}\alpha$ X-ray source. The XRD patterns were collected in a 2θ range of 5° to 65° with a counting time of 0.5 steps per second at a step size of 0.02° .

2.4 Electrochemical characterization

Electrochemical characteristics were studied using an EmStat2 potentiostat and ItalSens IS-C electrodes from PalmSens BV (The Netherlands). The potentiostat is a compact, portable, and economical instrument with a user-friendly interface, offering a wide range of features, including cyclic voltammetry, linear sweep voltammetry, and electrochemical impedance spectroscopy. The electrode, made of high-purity platinum, is of high quality and reliability, featuring a well-defined surface area.

The electrodes for electrochemical characterization were prepared by dropping 2 μL each of Sb@MXene, 5%Sb@MXene, and 25%Sb@MXene onto the surface of the electrode. The drop-cast solution was allowed to dry completely at room temperature for one day.

The electrochemical characteristics of both a bare screen-printed electrode (SPE) and modified SPEs were investigated using cyclic voltammetry (CV) with a ferri/ferrocyanide redox couple. This study aimed to explore the electrochemical behavior of each involved 1 mM ferri/ferrocyanide species in a 1 M NaCl buffer solution with each respective SPE. The potential range of the CV scan spanned from -0.2 V to $+0.6$ V for the ferri/ferrocyanide redox couple, utilizing various potential scan rates. This approach provides a detailed understanding of the electrochemical performance and stability of the modified SPE, laying the foundation for its potential applications in heavy metal detection.

2.5 Heavy metal detection using a Sb@MXene-modified SPE

Three heavy metal solutions (Pb, Cd, and Zn) were prepared at a concentration of 10 ppm using standard solutions. Each working solution of 60 μL was carefully dropped onto the Sb@MXene-modified SPE's surface. The deposition process was carried out at a potential of -1.4 V for 60 s, followed by a 3-second equilibration time. Square-wave voltammetric measurements were then conducted in

a potential range of -1.2 V to $+0.2$ V, with an incremental step of 0.4 mV. The frequency for these measurements was set at 50 Hz. This experimental setup enabled precise and controlled determination of heavy metal concentrations on the modified SPE.

3. Results and discussion

3.1 Structural and morphology characteristics of MXene and Sb@MXene

The crystalline structure studies of MAX (Ti_3AlC_2), pristine MXene, 5%Sb@MXene, 25%Sb@MXene composite and Sb samples were investigated using XRD technique. As shown in Figure 2, XRD pattern of MAX phase depicts the appearance of sharp peaks at 9.8° , 19.4° , 36.8° , 39.6° , and 42.5° , representing the diffraction peaks of (002), (004), (103), (104) and (105) planes of MAX phase (Ti_3AlC_2), respectively. Compared with that of MXene, the significant decrease of the Al (104) peak at $2\theta=39.6^\circ$ indicates the successful Al etching by HF to produce MXenes [20,21], which is primarily composed of titanium carbide (TiC). Additionally, the backshift of the 2θ at 9.8° to 6.3° after Al etching indicates the increase in d -spacing of the MXene sheets after etching process [11,22]. XRD patterns of the Sb@MXenes show the presence of sharper diffraction peaks compared with that of pristine MXenes, indicating the formation of well-crystallized composites after the hydrothermal process. As compared with XRD pattern of the Sb powder, that of both Sb@MXene composites exhibit distinct peaks at 25° and 29° , corresponding to the existence of (003) and (012) planes of Sb, respectively [23]. This implies the successful doping of Sb on the MXene structure. The 5%Sb@MXene and 25%Sb@MXene composite possessed nearly all the specific peaks of MXene and Sb, which confirmed the successful synthesis of the Sb@MXene composite. Besides, a little shift of peaks at 25° and 29° in the Sb@MXene is observed in the composite formation which could be attributed to the variation of lattice parameters in the final crystal structure.

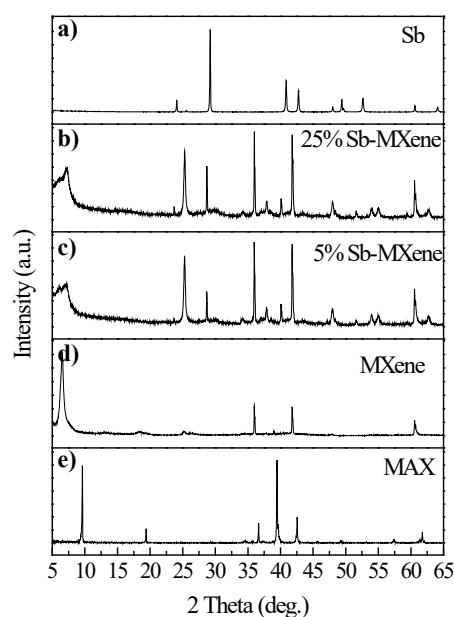
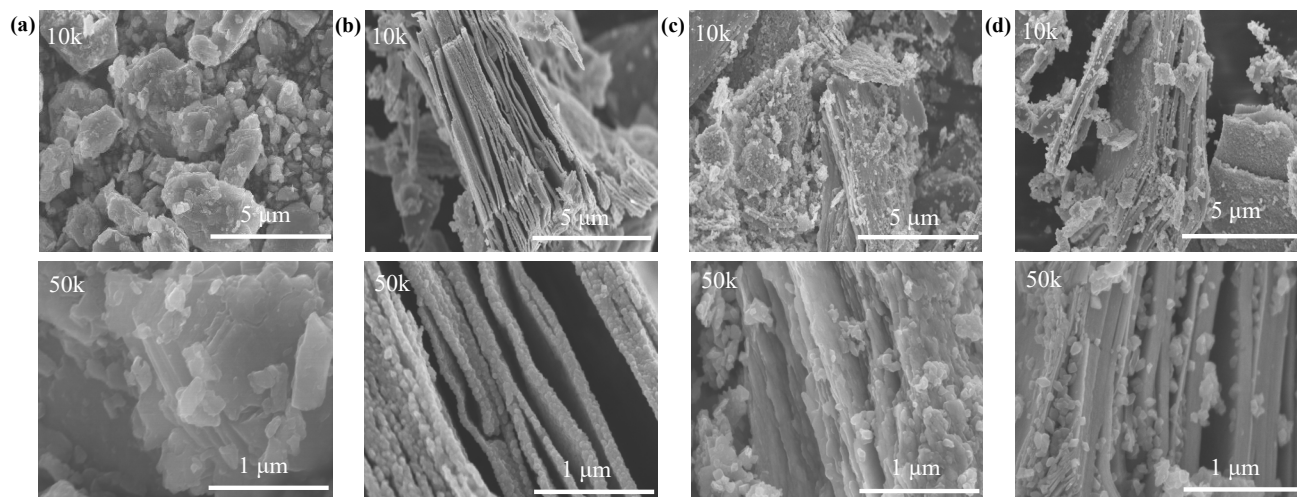


Figure 2. XRD patterns of (a) pure Sb powder, (b) 25% Sb@MXene, (c) 5%Sb@MXene, (d) MXene ($\text{Ti}_3\text{C}_2\text{T}_x$), and (e) MAX phase (Ti_3AlC_2).

Table 1. Elemental components of Sb powder, MAX phase, pristine MXenes, 5%Sb@MXene and 25%Sb@MXene from EDS technique.

Sample	%Atomic concentration					
	C	O	F	Al	Sb	Ti
Sb powder	22.88	3.35	0.00	5.77	67.65	0.36
MAX phase	40.77	13.02	0.00	8.58	0.08	37.55
Pristine MXene	29.01	31.78	9.56	0.76	0.05	28.84
5%Sb@MXene	15.45	49.09	2.52	0.76	1.11	31.07
25%Sb@MXene	14.96	22.01	1.32	2.17	4.16	55.37

**Figure 3.** SEM images using 10k and 50k magnifications of (a) MAX phase, (b) MXene, and (c) 5%Sb@MXene and (d) 25%Sb@MXene.

Surface morphology analysis by SEM image of MAX, MXene, 5%Sb@MXene, and 25%Sb@MXene samples are shown in Figure 3. The initial MAX precursor, prior to the chemical etching process, revealed a graphite-like multilayered closed packed sheet structure (Figure 3(a)). After the etching process, the larger spacing between each sheet is a clear indication that the Al layer has been effectively removed, resulting in the formation of 2D MXene nanosheets (Figure 3(b)). After doping Sb, SEM images of 5% and 25%Sb@MXene composite display a random distribution of Sb nanoparticles with the size of about 80 nm all over on the surface and interlayer of MXene sheets, indicating the successful preparation of the composite (Figure 3(c-d)). The Sb nanoparticles would be attached via the electrostatic interaction with the MXene sheets [24]. However, the 25%Sb@MXene composite exhibits slightly better distribution of Sb particles, whereas the 5%Sb@MXene composite show larger agglomeration of Sb particles which could affect to the electrochemical properties of materials.

Composition analyses of MAX phase (Ti_3AlC_2), Sb powder, MXene ($\text{Ti}_3\text{C}_2\text{T}_x$), and Sb@MXene composite obtained from EDX are shown in Table 1. The results show that the lower Al contents were found in the pristine MXene, 5%Sb@MXene, and 25%Sb-MXene compared with that of MAX precursor. The composition of the Sb-MXene composite confirms the increase in the Sb concentrations in accordance with the specified ratio. The small content of F in MXene and Sb-MXene composite is associated with the left over from etching process. The observed changes in the elemental composition, specifically the fluctuations in the content of Ti and O, can be attributed to the incorporation of antimony (Sb) into the MXene structure during the synthesis process. MXene, as a titanium carbide-based material,

inherently contains titanium (Ti) and carbon (C), with oxygen (O) also present due to surface oxidation. The elemental analysis presented in Table 1 confirms the presence of these elements in the synthesized composites. The observed decrease in the fluorine (F) content with increasing Sb concentration is consistent with the synthesis process. Fluorine, initially present in the pristine MXene from etching process with LiF, may be partially removed or replaced during the incorporation of Sb, leading to a decrease in the overall F content in the Sb@MXene composites. It's important to note that oxygen atoms can be absorbed on the MXene surface randomly, contributing to fluctuations in the oxygen content observed in the synthesized composites. The variations in elemental composition reflect the complex interplay between the synthesis conditions, the introduction of Sb dopant, and the inherent characteristics of the MXene structure.

3.2 Electrochemical characteristics

In this work, the electrochemical characterizations of bare SPE and 25%Sb@MXene-modified SPE were initially investigated using ferri/ferrocyanide redox couple. The cyclic voltammogram of the 25%Sb@MXene SPE exhibited a well-defined peak shape and higher peak current when compared with that of the bare SPE, illustrating the kinetic of electron transfer process on the modified electrode (Figure 4(a-b)). The oxidation peak potential (E_{pa}) and the reduction peak potential (E_{pc}) were at around +0.28 V and +0.03 V, respectively. In addition, to investing the mass transfer process of the modified electrode, cyclic voltammetry in ferri/ferrocyanide solution was carried out with the various potential scan rate (v) in the range of $10 \text{ mV}\cdot\text{s}^{-1}$ to $100 \text{ mV}\cdot\text{s}^{-1}$,

and the peak currents were then measured. The relationship between the anodic and cathodic peak current and the square root of scan rate were linear as shown in Figure 4(c-d). The Randles-Sevcik linear equations of the 25%Sb@MXene SPE were found to be $i_{pa} = 569.82v^{1/2} + 20.284$ with R^2 of 0.9908 and $i_{pc} = -699.58v^{1/2} - 8.0474$ with R^2 of 0.9938. The linearity of both anodic and cathodic current equation when using the 25%Sb@MXene SPE was greater than that of the bare SPE. Therefore, it was verified that the 25%Sb@MXene-modified SPE was able to apply for voltammetric sensing, and the mass transfer process was controlled by diffusion process.

3.3 Heavy metal detection using a Sb@MXene-modified SPE

The modified SPEs were applied to determine concentrations of three heavy metals including Pb^{2+} , Cd^{2+} , and Zn^{2+} by square-wave anodic stripping voltammetry. The deposition process was carried out at a potential of -1.4 V for 60 s, followed by a 3-second equilibration time. Square-wave voltammetric measurements were then conducted in a potential range of -1.2 V to $+0.2$ V, with an incremental step of 0.4 mV. The frequency for these measurements was set at 50 Hz. Figure 5 reveals that the stripping currents for Pb^{2+} , Cd^{2+} and Zn^{2+} were recorded at -0.50 V, -0.77 V, and -1.01 V, respectively. The results indicate that the 25%Sb@MXene-modified SPE exhibits higher sensitivity compared to the other modified electrodes, despite any

apparent visual similarities. Additionally, the baseline current of the electrodes should be considered when interpreting current response curves, as it can influence the apparent peak height. The sensitivity ratio was also calculated to compare the electrochemical sensing performance of 5% and 25%Sb@MXene electrodes (Table 2). The sensitivity ratio ($\mu A \cdot ppm^{-1}$) was calculated using peak current (μA) divided by metal ion concentration (ppm). Based on the sensitivity ratio value, 25%Sb@MXene-modified SPE exhibits the highest sensitivity ratio compared with other as-prepared SPE. This could be due to the enhancement of electrochemical activity from Sb-doping. The dispersion of Sb particles on MXene surface and interlayer could affect the electronic structure of the Sb@MXene composite, enhancing the kinetics of charge transfer [25]. Furthermore, a better dispersion of Sb particles on the MXene layer in the 25%Sb@MXene material would induce a greater electrochemical performance of the SPEs for metal ion detection in electrochemical sensor.

The 25%Sb@MXene-modified SPE was then selected to test the simultaneous determination of mixed solutions containing Pb^{2+} , Cd^{2+} , and Zn^{2+} compared with a blank solution as shown in Figure 6. It was found that the positions of stripping currents for Pb^{2+} , Cd^{2+} and Zn^{2+} were not significantly different from the determination in pure metal ion solution. This could confirm that the Sb@MXene-modified SPE has a great potential for use as electrochemical sensor in environmental monitoring application, especially the heavy metal sensing.

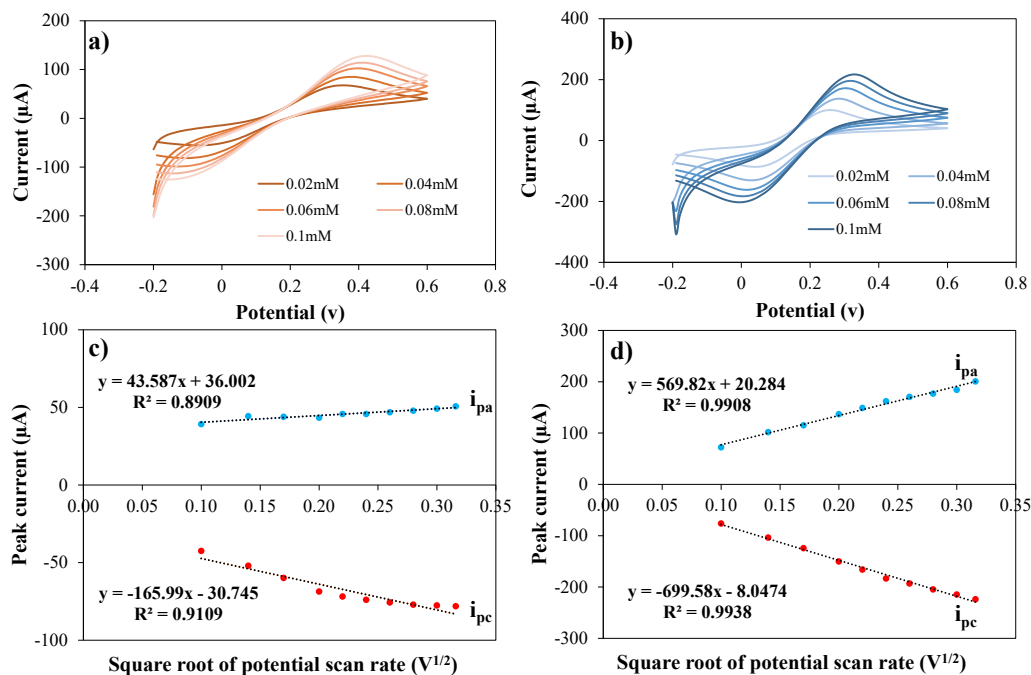


Figure 4. Cyclic voltammograms of ferrocyanide/ferricyanide redox couple using (a) a bare SPE, and (b) a 25%Sb@MXene-modified SPE, and relationship between peak current (i_p) and square root of potential scan rate ($v^{1/2}$) from the cyclic voltammograms of 1.0 mM ferri/ferrocyanide in 1.0 M NaCl with various potential scan rates on (a) a bare SPE and (b) a 25%Sb@MXene-modified SPE; where i_{pa} is anodic peak current and i_{pc} is cathodic peak current.

Table 2. Sensitivity ratio of 5%Sb@MXene- and 25%Sb@MXene-modified SPEs toward different metal ion at 10 ppm.

Electrode	Sensitivity ratio ($\mu A \cdot ppm^{-1}$)		
	Pb^{2+}	Cd^{2+}	Zn^{2+}
5%Sb@MXene-modified SPE	2.70	0.22	0.32
25%Sb@MXene-modified SPE	3.62	2.53	0.90

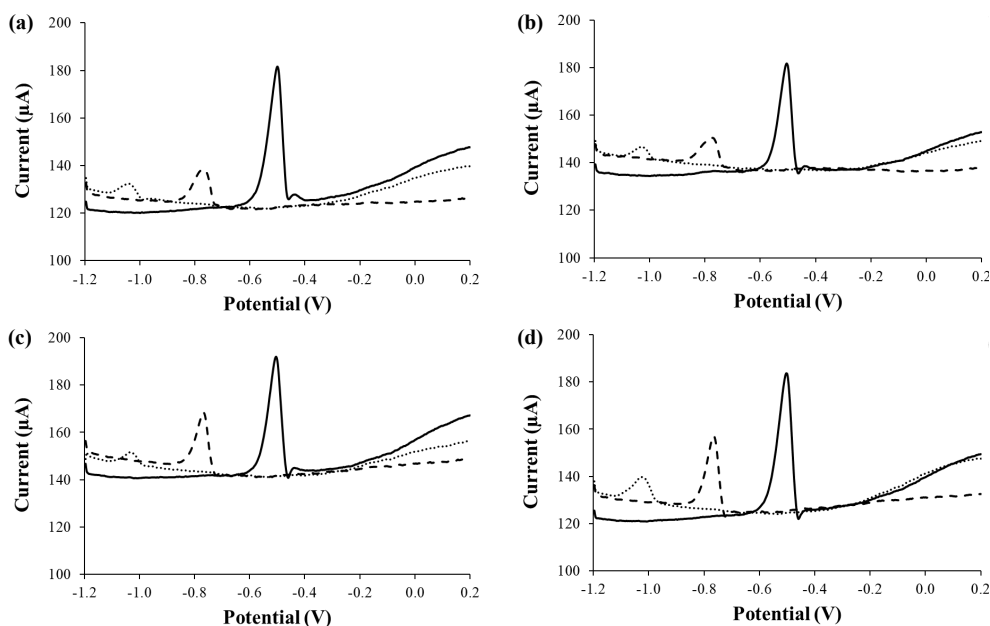


Figure 5. Square wave voltammograms of heavy metal solutions including Pb^{2+} (solid line), Cd^{2+} (dashed line), and Zn^{2+} (dotted line) by using (a) bare SPE, (b) MXene-modified SPE, (c) 5%Sb@MXene-modified SPE, and (d) 25%Sb@MXene-modified SPE.

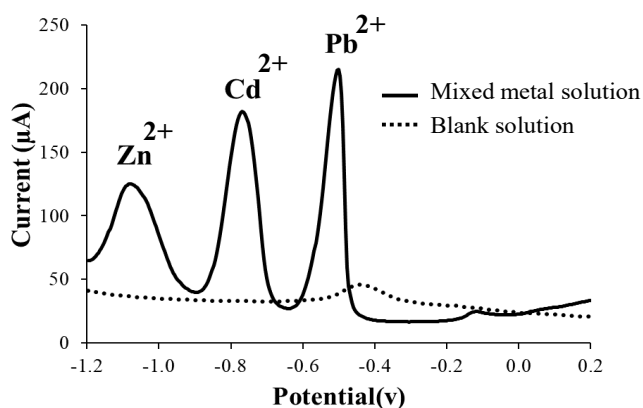


Figure 6. Typical square wave voltammograms showing the simultaneous determination of mixed solutions containing Pb^{2+} , Cd^{2+} , and Zn^{2+} (solid line) compared with a blank solution (dotted line), using a 25%Sb@MXene-modified SPE.

4. Conclusions

Herein, we have successfully developed novel titanium-based 2D materials, MXene, with antimony (Sb)-doped nanocomposites. These nanocomposites were fabricated using facile hydrothermal techniques, and their characteristics were assessed by measuring XRD, SEM, and EDS. Based on SEM-EDS results, the 25%Sb@MXene composite with the present of 4.1% Sb atomic concentration exhibited better dispersion of Sb nanoparticles on the surface and interlayer of MXene, compared with the 5%Sb@MXene. The Sb@MXene with different Sb ratios were utilized as a screen-printed electrode (SPE) material for heavy metal detection in electrochemical sensing application. The 25%Sb@MXene SPE exhibits the highest sensitivity toward Pb^{2+} , Cd^{2+} , and Zn^{2+} solutions due to a well dispersion of Sb nanoparticles on MXenes, and shows an ability to apply in simultaneous determination of mixed metal ion solutions. It's acknowledged that

a more thorough understanding of the relationship between Sb@MXene composition and its electrochemical properties would require studying a broader range of compositions. Expanding the study to include additional percentages of Sb@MXene would indeed provide a more comprehensive understanding and allow for a more nuanced analysis of the material's suitability for various applications. Future research endeavors could focus on exploring a wider range of compositions to further elucidate the role of Sb@MXene in electrode modification and its potential implications for heavy metal determination. The developed synthesis method and composite material would be able to further enlarge the electrochemical sensing for metal ion detection in practical environmental monitoring application.

Acknowledgements

This work was supported by the National Electronics and Computer Technology Center (NECTEC), and Department of Chemistry, Faculty of Science, Ramkhamhaeng University.

References

- [1] R. Wang, W. Young Jang, W. Zhang, C. Venkata Reddy, R. R. Kakarla, C. Li, V. K. Gupta, J. Shim, and T. M. Aminabhavi, "Emerging two-dimensional (2D) MXene-based nanostructured materials: Synthesis strategies, properties, and applications as efficient pseudo-supercapacitors," *Chemical Engineering Journal*, vol. 472, p. 144913, 2023.
- [2] M. Naguib, M. W. Barsoum, and Y. Gogotsi, "Ten years of progress in the synthesis and development of MXenes," *Advanced Materials*, vol. 33, no. 39, p. 2103393, 2021.
- [3] D. Ayodhya, "A review of recent progress in 2D MXenes: Synthesis, properties, and applications," *Diamond and Related Materials*, vol. 132, p. 109634, 2023.

- [4] M. P. Bilibana, "Electrochemical properties of MXenes and applications," *Advanced Sensor and Energy Materials*, vol. 2, no. 4, p. 100080, 2023.
- [5] P. Chakraborty, T. Das, and T. Saha-Dasgupta, "1.15 - MXene: A new trend in 2D materials science," in *Comprehensive Nano-science and Nanotechnology (Second Edition)*, D. L. Andrews, R. H. Lipson, and T. Nann Eds. Oxford: Academic Press, 2019, pp. 319-330.
- [6] A. Sohan, P. Banoth, M. Aleksandrova, A. Grace, and P. Kollu, "Review on MXene synthesis, properties, and recent research exploring electrode architecture for supercapacitor applications," *International Journal of Energy Research*, vol. 45, 2021.
- [7] U. Alli, K. McCarthy, I.-A. Baragau, N. P. Power, D. J. Morgan, S. Dunn, S. Killian, T. Kennedy, and S. Kellici, "In-situ continuous hydrothermal synthesis of TiO₂ nanoparticles on conductive N-doped MXene nanosheets for binder-free Li-ion battery anodes," *Chemical Engineering Journal*, vol. 430, p. 132976, 2022.
- [8] A. Dey, S. Varagnolo, N. P. Power, N. Vangapally, Y. Elias, L. Dampety, B. N. Jaato, S. Gopalan, Z. Golrokhi, P. Sonar, V. Selvaraj, D. Aurbach, and S. Krishnamurthy, "Doped MXenes—A new paradigm in 2D systems: Synthesis, properties and applications," *Progress in Materials Science*, vol. 139, p. 101166, 2023.
- [9] G. Qu, Y. Zhou, T. Wu, G. Zhao, F. Li, Y. Kang, and C. Xu, "Phosphorized MXene-phase molybdenum carbide as an earth-abundant hydrogen evolution electrocatalyst," *ACS Applied Energy Materials*, vol. 1, no. 12, pp. 7206-7212, 2018.
- [10] V. Thirumal, R. Yuvakkumar, P. S. Kumar, S. P. Keerthana, G. Ravi, M. Thambidurai, C. Dang, and D. Velauthapillai, "Facile hydrothermal synthesis of MXene@antimony nanoneedle composites for toxic pollutants removal," *Environmental Research*, vol. 210, p. 112904, 2022.
- [11] S. Arnold, A. Gentile, Y. Li, Q. Wang, S. Marchionna, R. Ruffo, and V. Presser, "Design of high-performance antimony/MXene hybrid electrodes for sodium-ion batteries," *Journal of Materials Chemistry A*, vol. 10, no. 19, pp. 10569-10585, 2022.
- [12] M. Alhabeab, K. Maleski, B. Anasori, P. Lelyukh, L. Clark, S. Sin, and Y. Gogotsi, "Guidelines for synthesis and processing of two-dimensional titanium carbide (Ti₃C₂T_x MXene)," *Chemistry of Materials*, vol. 29, no. 18, pp. 7633-7644, 2017.
- [13] Y. Guo, S. Jin, L. Wang, P. He, Q. Hu, L.-Z. Fan, and A. Zhou, "Synthesis of two-dimensional carbide Mo₂CT_x MXene by hydrothermal etching with fluorides and its thermal stability," *Ceramics International*, vol. 46, no. 11, Part B, pp. 19550-19556, 2020.
- [14] D. Mohanadas, R. Rohani, Y. Sulaiman, S. A. Bakar, E. Mahmoudi, and L.-C. Zhang, "Heavy metal detection in water using MXene and its composites: A review," *Materials Today Sustainability*, vol. 22, p. 100411, 2023.
- [15] E. Punrat, N. Piyasart, C. Auanphui, R. Thaipratum, S. Motomizu, and W. Wonsawat, "Sequential injection analysis for mercury ion with modified screen – printed carbon electrode," *Journal of Metals, Materials and Minerals*, vol. 32, no. 3, pp. 101-107, 2022.
- [16] P. Preechaburana, S. Sangnuy, and S. Amloy, "Paper-based colorimetric sensor for mercury ion detection using smartphone digital imaging," *Journal of Metals, Materials and Minerals*, vol. 33, no. 2, pp. 81-87, 2023.
- [17] E. Tesarova, L. Baldrianova, S. B. Hocevar, I. Svancara, K. Vytras, and B. Ogorevc, "Anodic stripping voltammetric measurement of trace heavy metals at antimony film carbon paste electrode," *Electrochimica Acta*, vol. 54, no. 5, pp. 1506-1510, 2009.
- [18] E. A. Shalaby, A. M. Beltagi, A. A. Hathoot, and M. A. Azzem, "Simultaneous voltammetric sensing of Zn²⁺, Cd²⁺, and Pb²⁺ using an electrodeposited Bi-Sb nanocomposite modified carbon paste electrode," *RSC Advances*, vol. 13, no. 11, pp. 7118-7128, 2023.
- [19] Y. He, L. Ma, L. Zhou, G. Liu, Y. Jiang, and J. Gao, "Preparation and application of bismuth/MXene nano-composite as electrochemical sensor for heavy metal ions detection," *Nanomaterials*, vol. 10, no. 5, p. 866, 2020.
- [20] M. Naguib, O. Mashtalir, J. Carle, V. Presser, J. Lu, L. Hultman, Y. Gogotsi, and M. W. Barsoum, "Two-dimensional transition metal carbides," *ACS Nano*, vol. 6, no. 2, pp. 1322-1331, 2012.
- [21] M. Naguib, M. Kurtoglu, V. Presser, J. Lu, J. Niu, M. Heon, L. Hultman, Y. Gogotsi, and M. W. Barsoum, "Two-dimensional nanocrystals produced by exfoliation of Ti₃AlC₂," *Advanced Materials*, vol. 23, no. 37, pp. 4248-4253, 2011.
- [22] R. Azadvari, S. Mohammadi, A. Habibi, S. Ahmadi, and Z. Sanaee, "Effect of ultra-sonication, vacuum drying, and carbon coating on the super-capacitive behavior of Ti₃C₂T_x MXene," *Journal of Physics D: Applied Physics*, vol. 57, no. 4, p. 045501, 2024.
- [23] W. Luo, S. Lorger, B. Wang, C. Bommier, and X. Ji, "Facile synthesis of one-dimensional peapod-like Sb@C submicron-structures," *Chemical Communications*, vol. 50, no. 41, pp. 5435-5437, 2014.
- [24] H. Yin, H. Tang, D. Wang, Y. Gao, and Z. Tang, "Facile synthesis of surfactant-free au cluster/graphene hybrids for high-performance oxygen reduction reaction," *ACS Nano*, vol. 6, no. 9, pp. 8288-8297, 2012.
- [25] X. Guo, H. Gao, S. Wang, G. Yang, X. Zhang, J. Zhang, H. Liu, and G. Wang, "MXene-based aerogel anchored with antimony single atoms and quantum dots for high-performance potassium-ion batteries," *Nano Letters*, vol. 22, no. 3, pp. 1225-1232, 2022.